AD-A071 758 CALIFORNIA UNIV BERKELEY ELECTRONICS RESEARCH LAB F/G 20/9
PLASMA THEORY AND SIMULATION.(U)
DEC 78 C K BIRDSALL N00014-77-C-0578
UNCLASSIFIED NL

| OF |
AD
A071758

END
DATE
FILMED
8-79
DDC

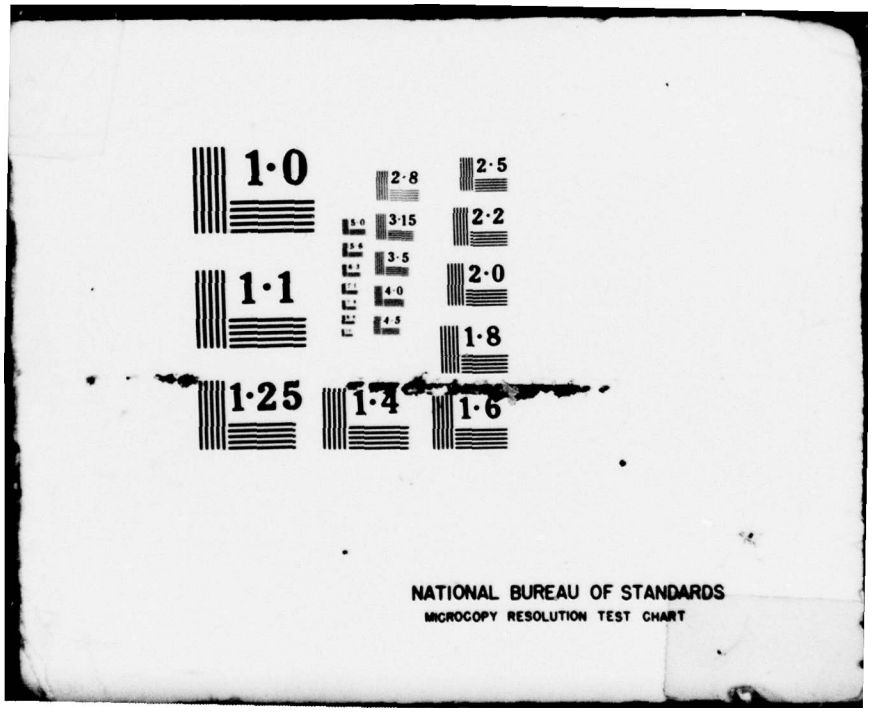
1·0
1·1
1·25
2·8
3·15
3·5
4·0
4·5
1·4
2·5
2·2
2·0
1·8
1·6
NATIONAL BUREAU OF STANDARDS
MICROCOPY RESOLUTION TEST CHART

LEVEL

12
B.S.

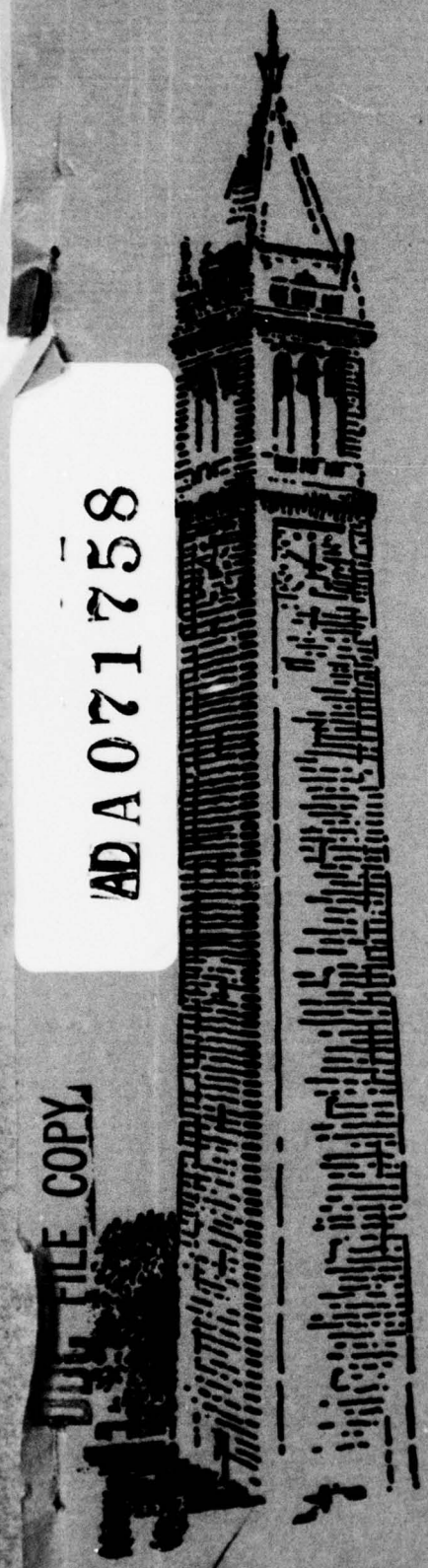

FOURTH QUARTER PROGRESS REPORT ON

PLASMA THEORY AND SIMULATION

October 1 - December 31, 1978

ERDA Contract EY-76-S-0034
(Project Agreement No. 128)

ONR Contract N00014-77-C-0578

ELECTRONICS RESEARCH LABORATORY
College of Engineering
University of California, Berkeley, CA 94720

NR.012-742
Code 421

FOURTH QUARTER PROGRESS REPORT

on

PLASMA THEORY and SIMULATION

October 1 — December 31, 1978

Research during the fourth quarter of 1978 is reported here.

Our research group uses both theory and simulation as tools in order to increase the understanding of instabilities, heating, transport, and other phenomena in plasmas. We also work on the improvement of simulation, both theoretically and practically.

Our staff is —

Professor C. K. Birdsall (Principal Investigator)	191	M	Cory Hall	(642-4015)
Alex Friedman (Post Doctorate)	119	ME	Cory Hall	(642-3477)
Yu Jiuan Chen, Douglas Harned, Jae Koo Lee, Lee Buchanan (Research Assistants)	119	MD	Cory Hall	(642-1297)
Stephen Au-Yeung (Programmer)	119	MD	Cory Hall	(642-1297)
Mike Hoagland Information Specialist	199	M	Cory Hall	(642-7919)

December 31, 1978

ERDA Contract EY-76-S-03-0034 (Project Agreement No. 128)
ONR Contract N00014-77-C-0578

ELECTRONICS RESEARCH LABORATORY
College of Engineering
University of California, Berkeley
94720

TABLE of CONTENTS

*Indicates ONR supported areas.

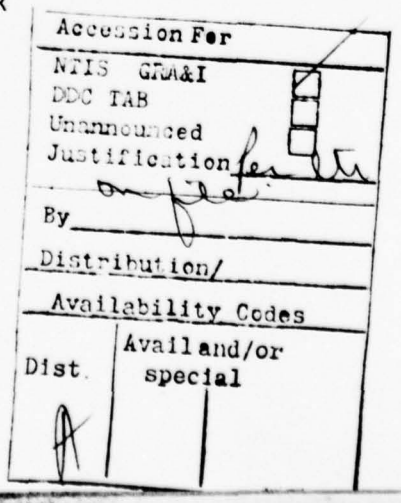

Section I
PLASMA THEORY

There are no additions to theory to report this quarter.

Section II
SIMULATION

A. DRIFT CYCLOTRON INSTABILITY PARTICLE SIMULATIONS

Jae Koo Lee (Prof. C. K. Birdsall)

The drift cyclotron instability (DCI) may occur in any finite collisionless magnetized plasma with a Maxwellian velocity distribution. The DCI may be a major confinement problem in most mirror machines, like 2XIIB or TMX, even after the DCLC mode is completely stabilized.

The many theoretical studies of DCI have not been very successful in providing uncontroversial information especially on the nonlinear evolution of this instability. We are using particle simulations to obtain linear and nonlinear behavior of this instability.

We have simulated DCI using an electrostatic 2-dimensional particle code, EZOHAR, for a Maxwellian velocity distribution, $f(v_\perp)$, with a density gradient in a uniform magnetic field. We use a slab model where the plasma density changes along only the x direction, and the magnetic field is along the z direction as in Fig. 1. The temperature is uniform, $T_s = 0$ $(s = e, i)$ and the electrons are cold initially $T_e = 0$; $T_i \neq 0$. The densities vary as

$$n_s(x_{gc}) = \begin{cases} n_o(1 + \epsilon_s \cos \kappa x_{gc}) & \text{for } x_{gc} \leq \pi/\kappa \\ 0 & \text{for } x_{gc} \geq \pi/\kappa \end{cases}$$

with Δ_i , Δ_e chosen to make $n_{eo} = n_{io}$. The system is periodic in y , bounded in the outer x , and has an inversion symmetry at the left x boundary (the zy plane).

As reported in the last QPR, our simulations produced linear growth rates in accordance with the ROOTS nonlocal theory. We will show detailed results for two mass ratios, namely, $m_i/m_e = 25$ and 100 , in an ERL Report in the next quarter.

The nonlinear evolution of this instability has been found to be complicated in single-mode simulations. We observed that the electrostatic field energy saturates at $1 \sim 2\%$ of the initial ion kinetic energy for most single-mode cases (of about 20 runs). The possible saturation mechanisms may be listed as:

(1) particle (electron or ion) trapping,
(2) nonlinear shift of the ion cyclotron frequency,
(3) wavebreaking (of electron or ion wave),
(4) electron (collisionless) heating, or
(5) the density gradient modification due to $\underset{\sim}{E}_x \times \underset{\sim}{B}$ drift.

Some of these mechanisms may be correlated with each other. We will present the details together with other nonlinear phenomena in the ERL Report.

B. LOWER-HYBRID DRIFT INSTABILITY SIMULATIONS USING AN ES1 HYBRID CODE

Yu-Jiuan Chen (Prof. C. K. Birdsall)

In the last QPR, according to Eqs. (3) and (4), the ions can be simply treated as unmagnetized particles. Assume ions are electrostatically confined, i.e., $\underline{v}_{yi} = \underline{v}_E + \underline{v}_i^* = 0$ where $\underline{v}_E$ is the $\underline{E} \times \underline{B}$ drift and $\underline{v}_i^*$ is the density gradient drift. Therefore, the "ghost" ion method[1] mentioned in the last report is not needed to simulate the lower-hybrid drift instability in the ions' frame.

The electrons are treated as a linearized fluid with susceptibility $\chi_e(k,\omega)$ to study the lower-hybrid drift instability. This method was originally used by Bruce Cohen and Gary Smith.[1] $\chi_e(k,\omega)$ is given by

$$\chi_e(k,\omega) = \frac{\omega_{pe}^2}{\omega_{ce}^2} \frac{1 - I_o(b)e^{-b}}{b} + \frac{\omega_e^2}{k_y^2 v_e^2} \frac{k_y v_*(k_y)}{\omega - k_y v_E} \qquad (1)$$

for a slab shape[2], where

$$b = k_y^2 \frac{T_e}{m_e \omega_{ce}} ,$$

$$v_*(k_y) = -\frac{T_e}{m_e \omega_{ce}} I_o(b)e^{-b} \frac{|\nabla n|}{n} , \qquad (2)$$

$\underline{v}_E$ is the $E \times B$ drift velocity, and ω_{pe}, ω_{ce}, m_e and T_e are the

[1] Bruce I. Cohen and Gary R. Smith, "Efficient Method for Local Simulation of Drift-Wave Instabilities", Proceedings of the Eighth Conf. on Numerical Simulation of Plasma, PD-8, 1978.

[2] R. C. Davidson and N. T. Gladd, "Anomalous Transport Properties Associated with the Lower-Hybrid-Drift Instability", Physics of Fluids, Vol. 18, No. 10, p. 1327 (1975).

electron plasma frequency, cyclotron frequency, mass and temperature, respectively.

The 1d Fourier transformed Poisson equation,

$$[1 + \chi_e(k,\omega)]\phi_k(t) = \frac{4\pi}{k^2}\rho_k(t) \tag{3}$$

may be written as

$$\left[1 + \left(\frac{\omega_{pe}}{\omega_{ce}}\right)^2 \frac{1 - I_o(b)e^{-b}}{b}\right]\left(i\frac{\partial}{\partial t} - kv_E\right)\phi_k + \frac{\omega_{pe}^2}{k^2 v_e^2} kv_*(k)\phi_k$$

$$= \frac{4\pi}{k^2}\left(i\frac{\partial}{\partial t} - kv_E\right)\rho_k \tag{4}$$

by replacing ω with the operator $i\frac{\partial}{\partial t}$, where ϕ_k and ρ_k are the perturbed potential and ion charge density. Put

$$A \equiv 1 + \frac{\omega_{pe}^2}{\omega_{ce}^2}\frac{1 - I_o(b)e^{-b}}{b}, \tag{5}$$

and

$$B \equiv \frac{\omega_{pe}^2}{2k^2 v_e^2} kv_* - A\frac{kv_E}{2}, \tag{6}$$

Eq. (4) is reduced to the form

$$iA\frac{\partial \rho_k}{\partial t} + 2B\rho_k = \frac{4}{k^2}\left(i\frac{\partial \rho_k}{\partial t} - kv_E\rho_k\right). \tag{7}$$

Using finite differences, we obtain

$$\frac{iA}{\Delta t}\left(\phi_k^{n+1} - \phi_k^n\right) + B\left(\phi_k^{n+1} + \phi_k^n\right) = \frac{4\pi}{k^2}\left[\frac{i}{\Delta t}\left(\rho_k^{n+1} - \rho_k^n\right) - \frac{kv_E}{2}\left(\rho_k^{n+1} + \rho_k^n\right)\right] . \tag{8}$$

Multiplying both sides by Δt , and setting

$$B' = B\Delta t \qquad \text{and} \qquad \frac{kv_E'}{2} = \frac{kv_E}{2}\Delta t , \tag{9}$$

Eq. (8) becomes

$$(iA + B')\phi_k^{n+1} + (B' - iA)\phi_k^n = -\frac{4\pi}{k^2}\left[\left(\frac{kv_E'}{2} - i\right)\rho_k^{n+1} + \left(\frac{kv_E'}{2} + i\right)\rho_k^n\right] . \tag{10}$$

Define

$$KSQI \equiv \frac{4\pi}{k^2} , \tag{11}$$

$$C_1 \equiv \frac{A^2 - B'^2}{A^2 + B'^2} , \tag{12}$$

$$C_2 \equiv \frac{2AB'}{A^2 + B'^2} , \tag{13}$$

$$C_3 \equiv KSQI \cdot \frac{A - B'\left(\frac{kv_E'}{2}\right)}{A^2 + B'^2} , \tag{14}$$

$$C_4 \equiv KSQI \cdot \frac{A\left(\frac{kv_E'}{2}\right) + B'}{A^2 + B'^2} ,$$

$$C_5 \equiv KSQI \cdot \frac{A + B' \frac{kv_E}{2}}{A^2 + B'^2} \quad , \tag{16}$$

and

$$C_6 \equiv KSQI \cdot \frac{A \frac{kv'_E}{2} - B'}{A^2 + B'^2} \quad . \tag{17}$$

Finally, we obtain

$$\phi_k^{n+1} = (C_1 + iC_2)\phi_k^n + (C_3 + iC_4)\rho_k^{n+1} + (-C_5 + iC_6)\rho_k^n \quad , \tag{18}$$

or

$$\text{Re } \phi_k^{n+1} = C_1 \text{ Re } \phi_k^n - C_2 \text{ Im } \phi_k^n + C_3 \text{ Re } \rho_k^{n+1} - C_4 \text{ Im } \rho_k^{n+1}$$

$$- C_5 \text{ Re } \rho_k^n - C_6 \text{ Im } \rho_k^n \quad , \tag{19}$$

$$\text{Im } \phi_k^{n+1} = C_1 \text{ Im } \phi_k^n + C_2 \text{ Re } \phi_k^n + C_3 \text{ Im } \rho_k^{n+1} + C_4 \text{ Re } \rho_k^{n+1}$$

$$- C_5 \text{ Im } \rho_k^n + C_6 \text{ Re } \rho_k^n \quad . \tag{20}$$

This code has been tried in the low-drift-velocity regime ($v_E < v_i$). Parameters used are $\omega_{pe}^2/\omega_{ce}^2 = 1$, $\omega_{pe}^2/\omega_{pi}^2 = m_i/m_e = 900$, $\omega_{pi}\Delta t = 0.04$, $N_{ion} = 1024$, $v_i = 0.141421$, $v_E = 0.04$, $v_e = 0.0$. The simulation result is shown in Fig. 1. The growth rate is on the order

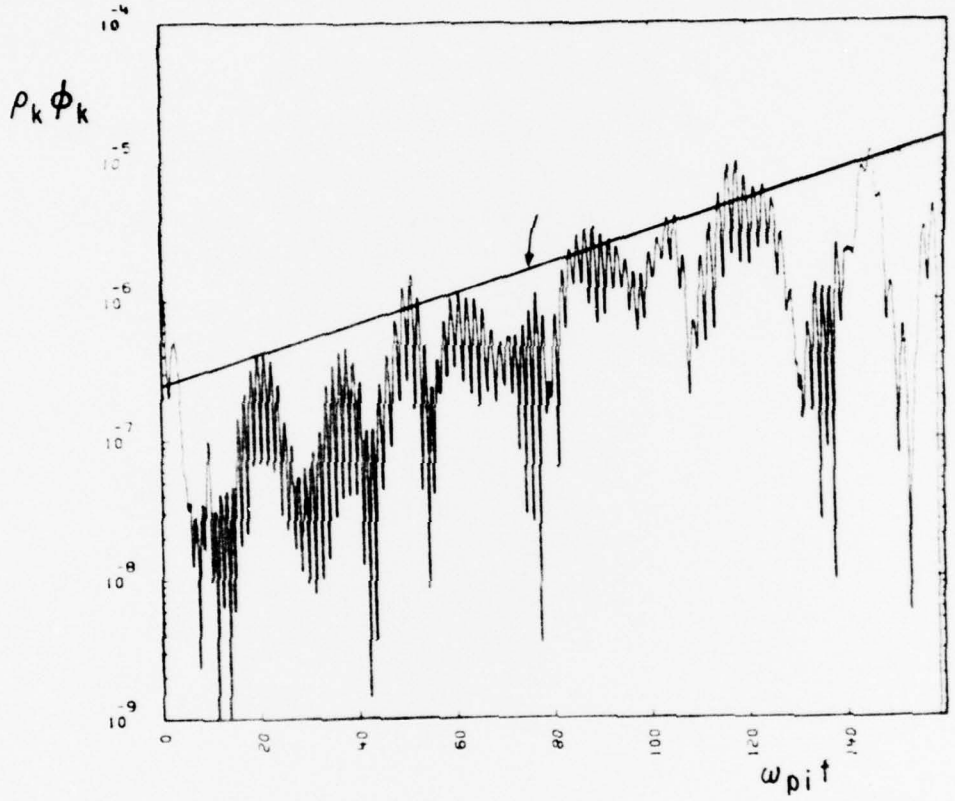
$\rho_k \phi_k$
10^{-4}
10^{-5}
10^{-6}
10^{-7}
10^{-8}
10^{-9}
0
20
40
60
80
100
120
140
$\omega_{pi} t$

FIGURE 1

of the theoretical value of Davdison[3]. B. I. Cohen (LLL) suggests use of smaller value of $(\omega_{pi}/\omega_{ci})^2$, and a larger number of particles, due to problems with multibeaming (numerical) instabilities; we will try these.

[3] R. C. Davisdon, "Quasi-Linear Stabilization of Lower-Hybrid-Drift Instability", Physics of Fluids, Vol. 21, No. 8, p. 1375 (1978).

C. FIELD REVERSED LAYER SIMULATIONS IN 2d

Douglas Harned (Prof. C. K. Birdsall, Alex Friedman)

During the past quarter we have been studying the two-dimensional electrostatic particle code EZOHAR with a view toward modifying it to simulate field-reversed layers (e.g., field-reversed mirror or field-reversing ion layer configurations). The simulations would thus be two-dimensional across the r-theta plane of the cylindrical field-reversed geometry. This type of simulation should enable us to examine the theory of Lovelace [1], as well as that of Uhm and Davidson [2], concerning the stability of long layers. When electron polarization effects are included (which will not be in the early stages of modification) it should also be possible to examine Ogden's[3] theory concerning the microstability of these systems, particularly the lower hybrid drift instability.

The theories of interest here are concerned with low frequency modes such as precession, for which low-frequency electromagnetic effects are important. Therefore our intent is to proceed by converting EZOHAR from an electrostatic to a Darwin model (i.e., neglecting radiation fields). Additionally the present particle code will be converted to a quasineutral hybrid one in which ions will be treated as particles and electrons will be treated as a fluid (in the initial modification, a massless fluid). This should be adequate for the frequencies of interest. The code will be

---

[1] R. V. Lovelace, "Precession and Kink Motion of Long Astron Layers", submitted to Physics of Fluids (1978).

[2] H. S. Uhm, R. C. Davidson, "Stability Properties of a Field-Reversed Ion Layer in a Background Plasma", PFC/JA-78-7 (1978).

[3] J. M. Ogden, "Analytic and Numerical Studies of Microinstabilities Driven by Ions", Ph.D. dissertation, Univ. of Maryland (1978).

nonlinear, and serve to complement linearized codes currently being developed (e.g., Friedman's[4] three dimensional hybrid code). Allowing nonlinearity may complicate observing and measuring linear growth rates between noisy starts and saturation; however, problems due to coarseness of initial conditions usually saturate at a low level in a nonlinear code, rather than grow indefinitely as in a linearized system. In addition, it should be of interest to observe saturation and other nonlinear effects on flute modes. This type of simulation is intended to provide valuable insight concerning the stability of field-reversed layers.

---

[4]A. Friedman, R. N. Sudan, J. Denavit, "A Linearized Hybrid Code for Stability Studies of Axisymmetric Field-Reversed Equilibria", Proceedings of the Eighth Conference on the Numerical Simulation of Plasmas, Monterey CA, June 1978.

Section III

CODE DEVELOPMENT and MAINTENANCE

A. ES1 ON THE CRAY

Stephen Au-yeung

1. Dial up number:

   Same as the A-machine

2. Logging in:

   c[user no] a 818sb1 (ctrl-z)[combo]

3. Getting ES1:

   ```
   rfilem   /  t  v
   *read  1222  .cray  es1/ℓ
   *end
   ```

4. Extracting files from es1/ℓ:

   ```
   lib es1/ℓ   /  t  v
   ok.  x  es1/s  es1  es1/b/ℓ
   ok.  end
   ```

   where

   es1/s is the FORTRAN source
   es1 is the executable file and
   es1/b/ℓ is the relocatable file library

5. Modifying ES1:

   ```
   qed es1/s   /  t  v
   - (qed commands)
   - end
   ```

6. Compiling and loading ES1:

   ```
   cft    i = es1/s,b = es1/b,ℓ = 0   /  t  v
   ldr    i = es1/b,x = es1,lib = es1/b/ℓ:tv80lib   /  t  v
   ```

7. Input file for ES1:

The name of the es1 input file is the string "input" followed by the current suffix (channel). For example, if suffix b is currently used, the name of the input file must be "inputb". This allows the capability of running up to 5 es1 programs simultaneously.

The input file specifies the problem, plots desired, etc. For example, a two-stream instability problem input could be:

```
box  b22  ee  stream    electron-electron two stream
nsp = 2     irho = 50     iphi = 50     ixvx = 25
mplot = 1 2 3     nt = 300
$
v0 = 1.     mode = 1     x1 = .001
$
v0 = -1.
$
```

For the meaning of those variables, see the INPUT section of the ES1 document written by Bruce Langdon.

8. Getting hardcopy output:

In order to get graphics from the nonimpact printer one has to first transfer his files to the A-machine. The procedure is as follows:

```
netout   a   alwith.   f105    b.
(crtl-d)  —  to logoff the Cray
(login under the A-machine)
nipit cfam. filename box bnn id    /  t  v
```

Note that no space in "id" is allowed and if the error message "The F0 ... file is missing" appears, ignore it.

B. EM1 Code

No special report.

C. EZOHAR DEVELOPMENT

W. M. Nevins and Y. Matsuda

We have tested EZOHAR, a bounded, 2d3v electrostatic plasma simulation code, by simulating a plasma slab in a uniform magnetic field. This slab is uniform in y. The plasma density is constant between $-L_x$ and L_x, and zero for $x > L_x$. This configuration was chosen for testing the code because the linear theory is relatively simple. Our goal in these tests are:

(1) To compare the normal mode frequencies with the linear theory, as this provides a test of the accuracy of the code in reproducing physics;

(2) To test the power of EZOHAR diagnostic package. In particular, we wish to demonstrate that the spatial structure of the normal modes can be obtained by examining the fluctuation spectra of a stable plasma.

We will first review the linear theory of the bounded plasma slab, and then present a summary of our simulation results to date.

A. *THE NORMAL MODES OF A BOUNDED PLASMA SLAB*

Within the plasma the normal modes vary spatially like sines and cosines. Hence, there are four linearly independent modes for each choice of k_x and k_y. We find it convenient to choose these four modes to be eigenfunctions of the inversion operator, and write them as

$$\Phi_1(x,y,t) = \Phi_1^{in} \cos k_x x \cos k_y y \cos(\omega t + \phi_1) \quad (1)$$

$$\Phi_2(x,y,t) = \Phi_2^{in} \sin k_x x \sin k_y y \cos(\omega t + \phi_2) \quad (2)$$

$$\Phi_3(x,y,t) = \Phi_3^{in} \sin k_x x \cos k_y y \cos(\omega t + \phi_3) \quad (3)$$

$$\Phi_4(x,y,t) = \Phi_4^{in} \cos k_x x \sin k_y y \cos(\omega t + \phi_4) \; . \quad (4)$$

Of these four wave forms, only Φ_1 and Φ_2 are even under inversion, i.e.,

$$\Phi_1(-x,-y,t) = \Phi_1(x,y,t) \quad (5)$$

and

$$\Phi_2(-x,-y,t) = \Phi_2(x,y,t) \; . \quad (6)$$

Hence, the inversion symmetry boundary condition imposed at $x = 0$ (see QPR of July 1, 1976) selects out modes Φ_1 and Φ_2, and rules out modes Φ_3 and Φ_4, which are odd under inversion.

For $x > L_x$, the normal modes must decay exponentially in x, i.e.,

$$\Phi_1(x,y,t) = \Phi_1^{out} \exp(-k_y x) \cos k_y y \cos(\omega t + \phi_1) \quad (7)$$

and

$$\Phi_2(x,y,t) = \Phi_2^{out} \exp(-k_y x) \sin k_y y \cos(\omega t + \phi_2) \; . \quad (8)$$

We will call Φ_1 the "cosine-like" mode, and Φ_2 the "sine-like" mode. Matching Φ and $\partial\Phi/\partial x$ at the boundaries, we find that

the cosine-like modes obey

$$\tan k_x L_x = k_y/k_x \tag{9}$$

while the sine-like mode obey

$$\cot k_x L_x = -k_y/k_x \ . \tag{10}$$

Periodic boundary conditions are imposed in y . Hence, k_y satisfies

$$k_y = \frac{2\pi}{L_y} m \quad , \quad m = 0,1,2 \ldots \tag{11}$$

Specializing to the case $L_x = L_y$, we find that cosine-like modes satisfy

$$z \tan z = 2\pi m \tag{12}$$

while the sine-like modes satisfy

$$z \cot z = - 2\pi m \quad , \quad m = 1,2,3 \ldots \tag{13}$$

where

$$a = k_x L_x \ . \tag{14}$$

Hence, the allowed values of $\underline{k}$ may be labeled by two integers: m is the number of nodes across the system in y , and n is the number of nodes across the system in x .

With the assistance of Miss Jean Yao we have solved Eqs. (12) and (13) numerically, with a rootsolver that employs the global Newton's method (see QPR of Oct. 1, 1977). These roots, together with

Eqs. (1) and (2), provide the allowed values of $|\underline{k}|$, which are shown in Tables I and II, and the normal mode structure, an example of which is shown if Fig. 1. The normal mode frequencies may then be obtained by solving the uniform plasma dispersion relation at these allowed values of $|\underline{k}|$. This is accomplished with Gerver's program UNIFORM[1], available from LIBRIS on the MFECC.

B. *ANALYSIS OF SIMULATION RESULTS; THE FREQUENCY AND STRUCTURE OF THE NORMAL MODES*

In our computer simulation runs we save time histories of the potential at fixed values of x k_y. The EZOHAR post-processor, ZED (see the previous QPR on ZED as used in ES1), then calculates the spectral density as a function of the discrete variables k_y and x, as well as the (essentially continuous) variable ω from these time histories. We identify the peaks in plots of the spectral density vs ω as the normal mode frequencies, while the amplitude of each peak is proportional to $|\Phi(x,k_y,\omega)|^2$. Hence, we may determine the spatial variation in the amplitude of the normal modes by plotting the spectral density vs x for fixed k_y and ω.

Figures 2a and 2b of the April 1978 QPR show typical plots of the spectral density vs ω. The upper-hybrid frequency and the electron gyroharmonics are clearly visible.

In general, we have found that the fluctuation is dominated by the long wavelength modes. Hence, those modes labelled with small values of m and n have greater amplitudes than those modes with larger

[1] M. J. Gerver, "ROOTS, A Dispersion Equation Solver", ERL Memo No. UCB/ERL M77/27, 31 Oct. 1976.

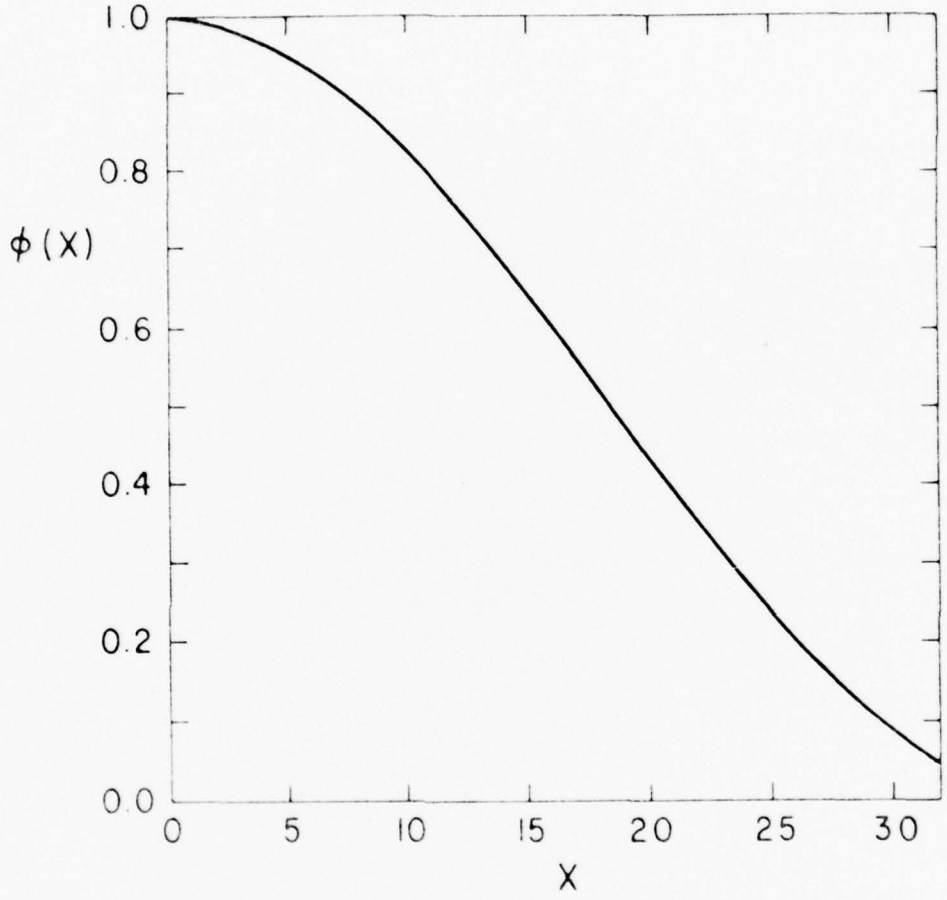

FIGURE 2

m and n values. We have, as yet, only been able to identify $n = 0$ mode structures by examining the fluctuation spectrum of a plasma slab in thermal equilibrium.

The technique described here may be easily generalized to obtain the spatial variation in the phase, as well as the amplitude, of the normal modes. This phase information is obtained from the cross-spectrum of the potential at different values of x. It should be easier to measure the spatial structure of an unstable mode (which will grow to large amplitude) than it is to pick the mode structure out of the thermal fluctuation spectrum. Hence, we expect that this technique will be very useful for comparing the normal mode structure observed in computer simulations with the results of linear normal mode calculations.

m \ n	1	2	3	4	5	6	7	8
real		3.14159	6.28319	9.42478	12.56637	15.70796	18.84956	21.99115
imag		0.	0.	0.	0.	0.	0.	0.
k		0.5	1.0	1.5	2.0	2.5	3.0	3.5
1	1.35795	4.13080	7.01370	9.18637	13.01610	16.08046	19.16634	22.26618
	0.	0.	0.	0.	0.	0.	0.	0.
	1.02309	1.19676	1.49868	1.87780	2.30031	2.74771	3.21015	3.68216
2	1.45549	4.37721	7.32616	10.30856	13.32257	16.36287	19.42379	22.50029
	0.	0.	0.	0.	0.	0.	0.	0.
	2.01337	2.11786	2.31507	2.58654	2.91477	3.28360	3.68194	4.10171
3	1.49182	4.47909	7.47638	10.48753	13.51512	16.55799	19.61506	22.68448
	0.	0.	0.	0.	0.	0.	0.	0.
	3.00938	3.08353	3.22736	3.43310	3.69145	3.99309	4.32965	4.69410
4	1.51076	4.53391	7.56173	10.59657	13.63993	16.69249	19.75221	22.82462
	0.	0.	0.	0.	0.	0.	0.	0.
	4.00722	4.00451	4.17713	4.34100	4.55111	4.80188	5.08169	5.40335
5	1.52238	4.56800	7.61614	10.66821	13.72527	16.78799	17.85669	22.93141
	0.	0.	0.	0.	0.	0.	0.	0.
	5.00587	5.05255	5.14483	5.28042	5.45635	5.66913	5.91502	6.19031
6	1.53023	4.59120	7.65368	10.71857	13.78657	16.85825	19.93396	23.01387
	0.	0.	0.	0.	0.	0.	0.	0.
	6.00494	6.04433	6.12240	6.23780	6.38862	6.57259	6.78714	7.02964
7	1.53589	4.60800	7.68108	10.75573	13.83246	16.91168	19.99364	23.07871
	0.	0.	0.	0.	0.	0.	0.	0.
	7.00427	7.03831	7.10595	7.20621	7.33803	7.49964	7.68700	7.90516
8	1.54017	4.62072	7.70194	10.75423	13.86797	16.95346	20.04097	23.13067
	0.	0.	0.	0.	0.	0.	0.	0.
	8.00375	8.03373	8.09337	8.18205	8.29889	8.44277	8.61241	8.80638

TABLE I. Cosine-like Modes: $z \tan z - 2\pi m = 0$

m \ n	1	2	3	4	5	6	7	8
real	1.57080	4.71239	7.85398	10.99557	14.13717	17.27876	20.42035	23.56194
imag	0.	0.		0.	0.	0.	0.	0.
k	0.25	0.75	1.25	1.75	2.25	2.75	3.25	3.75
	2.73151	5.55888	8.49104	11.49578	14.54494	17.62127	20.71455	23.81985
1	0.	0.	0.	0.	0.	0.	0.	0.
	1.09041	1.33519	1.68115	2.03500	2.41260	2.91746	3.44519	3.92072
	2.91375	5.84765	8.81316	11.81191	14.83980	17.89108	20.96042	24.04355
2	0.	0.	0.	0.	0.	0.	0.	0.
	2.05306	2.20594	2.44284	2.74483	3.09487	3.47965	3.88955	4.31778
	2.98456	5.97616	8.98018	11.99948	15.03468	18.08486	21.14834	24.22323
3	0.	0.	0.	0.	0.	0.	0.	0.
	3.03737	3.14717	3.32306	3.55030	3.83741	4.15747	4.50817	4.88497
	3.02193	6.04707	9.07815	12.11712	15.16505	18.22222	21.28838	24.36290
4	0.	0.	0.	0.	0.	0.	0.	0.
	4.02881	4.11415	4.25295	4.44062	4.67177	4.94074	5.24210	5.57089
	3.04497	6.09166	9.14161	12.19607	15.25589	18.32159	21.39331	24.47098
5	0.	0.	0.	0.	0.	0.	0.	0.
	5.02343	5.09313	5.20738	5.36356	5.55837	5.78817	6.04922	6.33786
	3.06059	6.12219	9.18577	12.25214	15.32193	18.39559	21.47338	24.55542
6	0.	0.	0.	0.	0.	0.	0.	0.
	6.01974	6.07860	6.17554	6.30892	6.47662	6.67620	6.90507	7.16054
	3.07186	6.14438	9.21818	12.29351	15.37174	18.45232	21.53582	24.62229
7	0.	0.	0.	0.	0.	0.	0.	0.
	7.01705	7.06795	7.15209	7.26831	7.41521	7.59109	7.79410	8.02227
	3.08039	6.16122	9.24293	12.32590	15.41048	18.49695	21.58553	24.67638
8	0.	0.	0.	0.	0.	0.	0.	0.
	8.01501	8.05981	8.13413	8.23701	8.36753	8.52446	8.70645	8.91203

TABLE II. Sine-like Modes: $z \cot z + 2\pi m = 0$

D. ES1 + EFL Code

Jae Koo Lee (Prof. C. K. Birdsall)

A journal article is in preparation for the *Journal of Computational Physics*.

E. RJET DEVELOPMENT

Stephen Au-Yeung (Alex Friedman)

The PDP-11/DMA Controller — model 121, the driver of the Versatec Printer, arrived in early November, 1978. However, while trying to install the controller, we found that there is no DD-11 DK Expanded Board left in the PDP-11/04 computer. Furthermore, the RJET software development group discovered that 16K words of additional memory was needed for the controller. Orders for the above-mentioned items have been placed and we are waiting for DEC people to deliver them.

F. RUNNING THE SAME PROGRAM SIMULTANEOUSLY UNDER DIFFERENT CHANNELS

Stephen Au-Yeung

Inserting the following code at the beginning of a program is an example of how to make the program run under different channels simultaneously:

```
parameter (nf = 3)
integer   fnames(nf)
data      fnames/8r    +prog,  84    input,  8r   output/
call setfile (fnames, nf)
call dropfile (fnames(1))
call open (5, fnames(2), 0, len)
call create (6, fnames(3), 1, -1)
```

where setfile is a subroutine that appends the current suffix to all names given in the array "fnames". To get this subroutine, type:

```
filem  rds  1222  .lib  flib  end    /   t  v
```

for the a-machine users, or type:

```
rfilem  read  1222  .cray  util/b/l  end    /   t   v
```

for the cray-1 users.

G. ROOTS IMPROVEMENT

Bruce Cohen and Neil Maron, LLL (A. Friedman and S. [illegible]-yeung)

A revised version of the ROOTS program has been developed by Bruce Cohen and Neil Maron at LLL with the capability of running a family of cases without the necessity of the user restarting the program for each case. To access the new version, type:

```
filem rds 3054 .root ro119a xroots cosout
```

The first of these files is the FORTRAN source, the second is the executable file, and the last is a sample cosmos deck for output processing.

To execute the new version, type: roots / t v
A sample terminal interaction session is as follows:

```
USER: xroots / 3 1.5
PROG:  type box and number (box lnn):
USER: box u22
PROG: input:
USER: more=1 jay=0 0 0 nspec=3 charg=1. 1. -1. ompsq=9. eps=.31 .31 .31
PROG: continue namelist input
USER: amass=1. 1. .00054437 dense=1.125 -.125 1. rlarm=1. .33333 0. end
PROG: input:
USER: more=0 eps=.29 .29 .29 end
PROG:  all done
```

The user sets more=1 if one or more case(s) will follow the current case, and more=0 if the current case is the last. Namelist input is terminated with "end".

The file cosout is a cosmos deck to send output to the versatec and fiche device, and should be modified to suit the user's needs - at least the box number must be changed. To process output, type:

```
cosmos i=cosout / t v
```

H. RINGHYBRID CODE; LOW DENSITY PLASMA CONSIDERATIONS

Alex Friedman

A. *INTRODUCTION*

The linearized, 3d hybrid code RINGHYBRID[1] was originally developed at Cornell University for the study of field-reversed ion ring stability in a dense cold background plasma. It is currently being supported by this author at U.C. Berkeley. The code follows the development in time of perturbations, with azimuthal mode number ℓ, about an axisymmetric zero-order state. The equilibrium current is purely azimuthal and is carried entirely by the energetic ion component, which is modeled by discrete particles in the code. [To zero order these are axisymmetric rings, while to first order they are perturbed in shape by a displacement $\xi \exp(i\ell\theta)$.] Alternately, discrete particles which are stationary to zero order can be initialized uniformly in space and the fluid ion component dispensed with. In addition, the cold background of ions and a complement of inertialess cold electrons, of density such that equilibrium charge neutrality obtains, are described by fluid equations.

One potential application of the code is to the study of field-reversed mirror plasmas. However, in this application the assumption of the existence of a uniform dense, cold plasma component is not appropriate. Thus, we need to examine the behavior of the RINGHYBRID algorithm when applied to equilibria containing regions where the density is low, and to consider modifications of the algorithm. We first discuss the present

---

[1] A. Friedman, R. N. Sudan, and J. Denavit, *Proc. of the Eighth Conference on Numerical Simulation of Plasmas*, Article PC-13, June 28-30, 1978, Monterey, California.

algorithm, and the nature of the limitation this algorithm imposes on the size of the timestep. A revision to the algorithm which eliminates this limitation is proposed. Finally, some considerations which arise when trying to generalize the model to one allowing regions of vacuum are presented.

B. *THE RINGHYBRID ALGORITHM; CONVERGENCE CRITERION FOR THE ITERATIVE SOLUTION OF OHM's LAW*

In this section we describe the algorithm presently employed in the solution of Ohm's Law, and the restriction imposed by this algorithm on the allowable timestep size, Δt . Defining dimensionless code variables as $B^\circ = \omega^\circ_{ci}\Delta t$, $n_i = \omega^2_{pi}\Delta x^2/c^2$, with similar units for other quantities (to eliminate Δt , Δx in the particle pusher and to simplify the algebra), omitting superscripts on first-order quantities, and letting a tilde (~) denote a quantity defined at the previous time level, Ohm's Law becomes

$$n_i \underline{E} = (\underline{B}^\circ/2) \times \nabla \times \nabla \times \underline{E} + \underline{W}' \ , \tag{1}$$

where

$$\underline{W}' \equiv (\underline{B}^\circ/2) \times \nabla \times \nabla \times \tilde{\underline{E}} + \underline{B}^\circ \times \underline{J}_i - \underline{B}^\circ \times \nabla \times \tilde{\underline{B}} \ . \tag{2}$$

Here $\underline{J}_i$ is due to the discrete ion component (we assume no fluid ion component present), and the last term in $\underline{W}'$ is obtained from $\int dt\ \nabla\times\nabla\times\underline{E}$.

The present version of RINGHYBRID solves Eq. (1) by direct iteration; dividing by n_i , $\underline{E}$ (in the left hand side) is set equal to the right hand side, which is itself a weak function of $\underline{E}$. This iteration

converges when $(\omega_{ci}^{\circ}\Delta t/2)(k^2c^2/\omega_{pi}^2) < 1$ (approximately). Assuming $k_{max}\Delta x = \pi$, in the dimensionless units employed this becomes

$$\pi^2 B^{\circ}/2n_i < 1 \ . \qquad (3)$$

Note that the Courant condition on Alfven waves restricts $B^{\circ}/\sqrt{n_i}$ to small values, so that as n_i decreases the convergence criterion for the direct iteration eventually imposes a more severe limit on Δt than does the Courant condition. Inhomogeneous mirror plasmas will contain regions of small n_i, so that an undesirably small Δt must be chosen if the present algorithm is used.

C. *A PROPOSED MODIFICATION TO FACILITATE INVERSION OF OHM'S LAW IN PROBLEMS INVOLVING SMALL* n_i

To eliminate the restriction imposed by direct iteration on (1) it is necessary to bring the term $(\underline{B}^{\circ}/2) \times \nabla \times \nabla \times \underline{E}$ to the left hand side. Since $\underline{B}^{\circ}$ and n_i are functions of the spatial variable z a direct inversion by Fourier analysis in z and tridiagonal solution in r is not feasible; a form of ICCG inversion would be suitable, but for simplicity a simpler iterative method is proposed. This would replace the direct iteration on (1).

Equation (1) represents six equations for the unknown components of $\underline{E}$, since E_r, E_θ, E_z each have 2 parts, $E^c \propto \cos \ell\theta$ and $E^s \propto \sin \ell\theta$, where ℓ is the azimuthal mode number. Thus, in each cell (i,j) we have a 6×6 matrix to invert for $\underline{E}_{ij}$, assuming $E_{i,j+1}$, $E_{i+1,j}$, ... known. For example, the first equation (for the ^c_r component) is, letting $\alpha = \Delta r/\Delta z$

$$n_i E^c_{rij} - \frac{B^o_{zij}}{2}\left[(\ell/r_j^2)E^s_{rij} - (2+2\alpha^2+1/r_j^2)E^c_{\theta ij}\right]$$

$$= W'^c_{rij} - \frac{B^o_{zij}}{2}\left\{(\alpha\ell/2r_j)(E^s_{z_{i+1,j}} - E^s_{z_{i-1,j}})\right.$$

$$- \alpha^2(E^c_{\theta_{i-1,j}} + E^c_{\theta_{i+1,j}}) - (1+1/2r_j)\,E^c_{\theta_{i,j+1}}$$

$$\left. - (1-1/2r_j)\,E^c_{\theta_{i,j-1}} + (\ell/2r_j)(E^s_{r_{i,j+1}} - E^s_{r_{i,j-1}})\right\}$$

$$\equiv X^c_{rij} \,. \qquad (4)$$

Similarly, the other 5 component equations are found, yielding an equation of the form

$$\begin{bmatrix} & & & & & \\ & & & & & \\ & & \overleftrightarrow{A} & & & \\ & & & & & \\ & & & & & \end{bmatrix} \begin{bmatrix} E^c_{rij} \\ E^s_{rij} \\ E^c_{\theta ij} \\ E^s_{\theta ij} \\ E^c_{zij} \\ E^s_{zij} \end{bmatrix} = \begin{bmatrix} X^c_{rij} \\ X^s_{rij} \\ X^c_{\theta ij} \\ X^s_{\theta ij} \\ X^c_{zij} \\ X^c_{zij} \end{bmatrix} . \qquad (5)$$

The "$\underline{E}_{i,j+1}$", etc. parts of $\underline{X}$ already appear in the current version of RING-HYBRID, and only the "$\underline{E}_{ij}$" terms need be deleted from the source terms in the present code. Explicitly, we find $\overleftrightarrow{A}$ to be, omitting indices i,j and letting $b = B^o_{ij}/2$

$$\overleftrightarrow{A} =$$

$$\begin{bmatrix}
n_i & -b_z \ell/r^2 & b_z(2+2\alpha^2+1/r^2) & 0 & 0 & 0 \\
b_z \ell/r^2 & n_i & 0 & b_z(2+2\alpha^2+1/r^2) & 0 & 0 \\
-b_z(2\alpha^2+\ell^2/r^2) & 0 & n_i & -b_z \ell/r^2 & b_r(2+\ell^2/r^2) & 0 \\
0 & -b_z(\ell^2/r^2+2\alpha^2) & b_z \ell/r^2 & n_i & 0 & b_r(2+\ell^2/r^2) \\
0 & b_r \ell/r^2 & -b_r(2+2\alpha^2+1/r^2) & 0 & n_i & 0 \\
-b_r \ell/r^2 & 0 & 0 & -b_r(2+2\alpha^2+1/r^2) & 0 & n_i
\end{bmatrix} .$$

(6)

This matrix is singular for $n_i = 0$, and ill-conditioned when n_i is very small; to see this note the linear dependence of the first and fifth rows when $n_i = 0$. Inverting this matrix gives E^c_{rij}, E^s_{rij}, ... as a function of $\underline{W}'_{ij}$ and the $E^c_{ri,j+1}$, ... , which are assumed "known" from the last pass in the iterative scheme proposed. This inversion should be done once, on paper, and $\overleftrightarrow{A}^{-1}$ programmed into the code.

While this modification does not change the model equations at all, and hence in principle does not alter the range of problems for which the model equations provide a reasonable description, the relaxation of the restriction on Δt should make practical the simulation of inhomogeneous mirror plasmas.

D. GENERALIZATION TO PROBLEMS INVOLVING VACUUM REGIONS

A possible generalization of the code involves matching the plasma model (with either direct iteration or the above method) to a vacuum region, where the equation $\nabla^2 \underline{E} = 0$ is assumed to hold. Note that specification of $\nabla \times \nabla \times \underline{E} = 0$ in vacuum is by itself insufficient. The additional specification of $\nabla \cdot \underline{E} = 0$ or at least $\nabla(\nabla \cdot \underline{E}) = 0$ is necessary to determine all components of $\underline{E}$. Combining $\nabla \cdot \underline{E} = 0$ with $\nabla \times \nabla \times \underline{E} = 0$ yields $\nabla^2 \underline{E} = 0$ as the equation to be solved.

The author has, for a previous version of the 3d linearized code, developed an iterative solver for the equation $\nabla^2 \underline{A} = \underline{J}$; with a change of notation this is directly applicable to the solution of $\nabla^2 \underline{E} = 0$. Explicitly, in "vacuum" cells (possibly defined to be those cells where, say, $v_{Alfven} \Delta t / \Delta x > 0.5$), we solve

$$S_{1ij} - UCR_j E^c_{rij} - UCX_j E^s_{\theta ij} = 0$$

$$S_{2ij} - UCR_j E^s_{\theta ij} - UCX_j E^c_{rij} = 0 \qquad (7)$$

where $UCR_j \equiv 2+2\alpha^2+\ell^2/r^2+1/r^2$, $UCX_j \equiv 2\ell/r_j^2$, and S_1 , S_2 come from cells of the unknown other than i,j , and from a source term taken to be zero for the current application. We solve to find

$$E^c_{rij} = (UCR_j S_{1ij} - UCX_j S_{2ij}) \Big/ (UCR^2_{ij} - UCX^2_{ij})$$

$$E^s_{\theta ij} = UCR \leftrightarrow UCX \tag{8}$$

and similarly for the other components.

However, it remains to be determined whether the solution to this equation in vacuum implies a smooth transition from the solution to Eq. (1) in plasma. In a private communication, J. Byers suggests that in the last plasma cells or first vacuum cells strong "sheath" effects may be present. Some observations relevant to this issue follow.

Where $n_i = 0$, the plasma Eq. (1), Ohm's Law, makes little physical sense. However, formally it reduces to

$$- \underline{B}^\circ \times \nabla \times \nabla \times (\underline{E} + \tilde{\underline{E}})/2 = - \underline{B}^\circ \times \nabla \times \tilde{\underline{B}} \ , \tag{9}$$

i.e.,

$$\underline{B}^\circ \times \nabla \times \underline{B} = 0 \ , \tag{10}$$

or,

$$B^\circ \times \nabla \times \nabla \times \underline{E} = 0 \tag{11}$$

with proper choice of initial conditions. This last is certainly true, and is a "subset" of $\nabla \times \nabla \times \underline{E} = 0$, but evidently is not sufficient to specify $\underline{E}$ in vacuum (even when n_i is nonzero but very small, problems are likely to be present). Consider the 1d , radial-variation-only limit: Eq. (1) becomes

$$\hat{r}: \quad n_{ij}E_{rj} + bz_j(2 + 1/r_j^2)E_{\theta j} = W'_{rj} + b_z\left((1+1/2r_j)E_{\theta,j+1} + (1-1/2r_j)E_{\theta,j-1}\right) \quad (12a)$$

$$\hat{\theta}: \quad n_{ij}E_{\theta j} = W'_{\theta j} = B^{o}_{zj}J_{irj} \quad (12b)$$

The latter of these gives $E_{\theta j} = B^{o}_{zj}\, J_{irj}/n_{ij}$, which is a badly posed equation when n_i is small since J_{ir} will fluctuate due to the small number of particles/cell (n_i is assumed "frozen", as it is a zero-order quantity). With E_θ so specified, $J_{\theta TOTAL}$ is specified and hence E_r is determined. In vacuum,

$$(2 + 1/r_j^2)\underline{E}_j = (1 + 1/2r_j)\underline{E}_{j+1} + (1 - 1/2r_j)\underline{E}_{j-1}\,, \quad (13)$$

the same equation holding for both components E_r and E_θ. Even though n_i may be small in (12a), n_iE_r may not be, and in any event E_θ is determined by (12b). Thus, the vacuum and plasma equations do not appear at all similar; only the latter supports waves, and the interface must reflect these waves in some manner, so that sheath effects are likely. Appropriate jump conditions at the interface must thus be formulated. These questions are undergoing further study.

E. *CONCLUSIONS*

In its present form the RINGHYBRID code is applicable to a restricted class of problems involving dense plasmas which are spatially nearly homogeneous. A modification has been proposed which would facilitate modeling of more strongly inhomogeneous mirror plasmas, as in field-reversed mirror configurations. Finally, some considerations which arise when one attempts to generalize the model itself to include vacuum regions have been presented.

Section IV
PLASMA SIMULATION TEXT

Our 800+ pages of notes have been edited and redone, with contents as below. The new chapters 6,7,12,13,14,15,16, and the Appendices. The set is available from Prof. Birdsall. Send a check for $23.75 (our cost) made out to Regents, University of California. The printing was limited; first come, first serve.

PLASMA PHYSICS via COMPUTER SIMULATION

by

Charles K. Birdsall and A. Bruce Langdon

Part I PRIMER

One Dimensional Electrostatic and Electromagnetic Codes

Chapter 1. Some ideas on why computer simulation using particles makes good physical sense.
2. Over-all view of a 1d electrostatic program.
3. A 1d electrostatic program, ES1.
4. Introduction to the numerical methods used.
5. Projects for ES1.
6. A 1d electromagnetic program, EM1.
7. Projects for EM1.

Part II THEORY

Plasma Simulation Using Particles in Spatial Grids with Finite Time Steps; Warm Plasma

8. Effects of the spatial grid.
9. Effects of the finite time step.
10. Energy conserving simulation models.
11. Dipole models.
12. Kinetic theory for fluctuations and noise.
13. Statistical mechanics of a sheet plasma.

Part III PRACTICE

Programs in Two and Three Dimensions; Design Procedures

14. Electrostatic Programs in 2d, 3d.
15. Electromagnetic programs in 2d, 3d.
16. Design of computer experiments; choice of parameters.

Part IV
Appendices

DECEMBER 1978

Section V
SUMMARY OF REPORTS, TALKS AND PUBLICATIONS IN THE PAST QUARTER

J. K. Lee and C. K. Birdsall

"VELOCITY SPACE RING-PLASMA INSTABILITY, MAGNETIZED: PART I, THEORY; PART II, SIMULATION"

(Submitted to Physics of Fluids)

DISTRIBUTION LIST

Contractor (DOE)
Robert Price
Donald Priester
Walter Sadowsky
Oscar Manley

Contractor (ONR)
Padgett (plus 67 to ONR list), Keith, Grisham

Berkeley Campus
Birdsall, Chen, Harned, Buchanan, Lee, Lichtenberg, Lieberman, Arons, McKee, Chorin, Au-Yeung, Friedman

Berkeley Lab (LBL)
Kunkel, Kaufman, Cooper, Maria Feder (library), Pyle

Livermore (LLL)
Byers, McNamara, Maron, Kruer, Langdon, Lasinski, Max, Fuss, Bruijnes, Tull Killeen, Marx, Mirin, Fries, Harte, Cohen, Taylor, CTR Library, Berk Briggs, Lee, Chambers, Smith, Matsuda

Israel
Gell, Cuperman

U.C. Davis
DeGroot

Univ. of Maryland
Guillory, Sternlieb

U.C.L.A.
Dawson, Lin

Univ. of PA
Fawley

Stanford
Buneman, Barnes

Columbia Univ.
Chu

Princeton PPL
Chen, Okuda, Graydon (Library), Nevins, Tang

Oak Ridge NL
Meier, Dory, Mook (Library)

Los Alamos SL
Lindman, Nielson, Burnett (Library) Gitomer, Lewis, Hewett, Forslund, Godfrey

Stevens Inst.
Rosen

Berkeley Space Sciences Lab
Hudson, Potter

ITT-Spain
Canosa

U.C.-Irvine
Rynn

NASA
Hohl

Kirtland AF3
Pettus

Northwestern Univ.
Denavit

Naval Research Lab
Boris, Winsor, Lee

SAI
Klein, McBride, Wagner

IBM Palo Alto
Gazdag

EPRI
Gough, Scott

General Atomic
Helton, Tommey (Library)

Univ. of Reading
Hockney

Inst. fur Plasmaphysik
Biskamp

Bell Labs
Hasegawa

Culham Lab
Roberts, Eastwood

Plasma Physics Inst. Nagoya
Kamimura

MIT
Bers, Berman

NYU
Grad

Univ. of Wisconsin
Shohet

Univ. of Texas
Macmahon, Horton

Univ. of Iowa
Knorr, Joyce, Nicholson

Cornell Univ.
Gerver

Univ. Rochester
Albritton

Sandia Laboratories
Freeman, Poukey

Bhabha Atomic Research Centre
R.N. Aiyer

Mission Research Corp
W. E. Hobbs
C. E. Rathmann

NOTE: Please send advice on additions/deletions to Prof. C.K. Birdsall. If you want your copy or an additional copy to be sent to your library, please send complete address.